

# Crystalline-State Reaction of Cobaloxime Complexes. 18.<sup>1)</sup> Metastable Intermediate Structure Observed by a New X-Ray Diffractometer for Rapid Data Collection

Yuji Ohashi,\* Yoshii Sakai, Akiko Sekine, Yoshifusa Arai,<sup>†</sup> Yoshiaki Ohgo,<sup>†</sup>  
Nobuo Kamiya,<sup>††</sup> and Hitoshi Iwasaki<sup>††</sup>

Department of Chemistry, Tokyo Institute of Technology, Ookayama, Meguro-ku, Tokyo 152

<sup>†</sup> Niigata College of Pharmacy, Kamishin'ei-cho, Niigata 950-21

<sup>††</sup> The Institute of Physical and Chemical Research (Riken), Wako, Saitama 351-01

(Received April 18, 1995)

A crystal of [(*R*)-1,2-bis(methoxycarbonyl)ethyl]bis(dimethylglyoximate)(diphenylmethylphosphine)-cobalt(III) changes its cell dimensions with retention of the single crystal form on exposure to visible light. The change is so fast that a new type of diffractometer (IPD-WAS) was developed for rapid data collection. The structures were analyzed at four different stages of the change using the diffractometer, which enabled us to collect the three-dimensional intensity data within 2 h. The cell dimensions of the monoclinic crystal varied from  $a=13.678(2)$ ,  $b=24.880(6)$ ,  $c=9.391(2)$  Å,  $\beta=107.99(1)^\circ$ , and  $V=3040(1)$  Å<sup>3</sup> to  $a=13.56(1)$ ,  $b=25.06(1)$ ,  $c=9.381(6)$  Å,  $\beta=107.35(6)^\circ$ , and  $V=3044(3)$  Å<sup>3</sup>. The space group was changed from  $P2_1$  to  $P2_1/n$ . The structures at four stages showed that there are two crystallographically independent molecules, A and B, in an asymmetric unit of the crystal before irradiation and that the chiral 1,2-bis(methoxycarbonyl)ethyl (bmce) group of the B molecule is completely inverted to the opposite configuration while the chiral bmce group of the A molecule remains unaltered after irradiation. This brings about an inversion center between the two molecules. The reaction cavity for the B bmce group is significantly greater than that for the A bmce group. At the intermediate stages, the B bmce group takes complicated disordered structures, which indicates that there exists a metastable intermediate structure in the inversion process.

It has been found that the chiral 1-cyanoethyl (ce) group,  $-\text{C}^*\text{H}(\text{CH}_3)\text{CN}$ , bonded to the cobalt atom of some bis(dimethylglyoximate)cobalt(III), cobaloxime, complexes is racemized by X-ray exposure with retention of the single crystal form.<sup>2)</sup> The rate of racemization was so slow that several intermediate structures were obtained by X-ray analysis. The gradual inversion of the chiral ce group was directly observed by the change on the electron density map.<sup>3)</sup> When the axial base ligand was replaced with other amines or phosphines, a variety of racemizations have been observed.<sup>4)</sup> We have defined the reaction cavity for the reactive group.<sup>5)</sup> The size of the reaction cavity explains not only the difference in various modes of racemization but also a wide variety of the reaction rates.<sup>6)</sup>

When the chiral group was replaced with the bulky 1-methoxycarbonyl ethyl (mce) group,  $-\text{CH}^*(\text{CH}_3)-\text{CO}_2\text{CH}_3$ , the racemization was observed only at high temperatures for the complexes with 4-chloropyridine and pyridine as axial base ligands. For the 4-chloropyridine complex, the inversion of the mce group was accompanied by a conformational change.<sup>7)</sup> For the pyridine complex the crystal has a solvent methanol

molecule in an asymmetric unit, which goes out from the crystal at room temperature following the conformational change of the mce group. The configuration of the chiral mce group is retained at this stage. The configurational change was observed at 343 K. Since the Co–C bond may be cleaved by X-ray exposure even at room temperature, these results suggest that the conformational change should be easier than the configurational change in the crystal lattice at room temperature.<sup>8)</sup>

Recently a series of the cobaloxime complexes with a bulkier chiral group, 1,2-bis(methoxycarbonyl)ethyl (bmce) group,  $-\text{C}^*\text{H}(\text{CO}_2\text{CH}_3)\text{CH}_2\text{CO}_2\text{CH}_3$  were prepared by two of us (Y. Ohgo and Y. Arai).<sup>9)</sup> Powdered samples suspended in an insoluble liquid were irradiated with visible light at room temperature. The optical rotation gradually decreased with irradiation time. One of the complexes, which has diphenylmethylphosphine (dpmp) as an axial base ligand, bmce–dpmp, had a racemization rate as large as those of the ce complexes which showed crystalline-state racemization.<sup>9)</sup> This suggested the idea that the crystals of the bmce–dpmp complex may be racemized with retention of the sin-

gle crystal form. Preliminary experiments showed that the cell dimensions changed very rapidly on exposure to the room light, although the bmce group is much bulkier than the ce or mce group. Since the chiral group was mostly racemized during the collection of the three-dimensional intensity data, a new diffractometer for rapid data collection (IPD-WAS) has been developed to analyze the structure at the initial and several intermediate stages.<sup>10</sup> The stepwise structure analyses showed that there must be a metastable intermediate species in the process of the inversion. This paper reports these quite new findings of a crystalline-state reaction using a new type of diffractometer. Another bmce complex with pyridine as an axial base ligand (bmce-py) also showed crystalline-state racemization on exposure to visible light. Although the mode of the racemization is similar to the bmce-dpmp complex, the precise analysis was very difficult.<sup>11</sup> The structures of three other bmce complexes with different axial base ligands, *R*(+)-phenylethylamine, (bmce-*R*-pea),<sup>12</sup> *S*(-)-phenylethylamine (bmce-*S*-pea),<sup>11</sup> and propylamine (bmce-pa),<sup>11</sup> which showed no reactivity, have been reported.

### Experimental

The bmce-dpmp complex was prepared in a way similar to that reported previously<sup>13</sup> and the details of the preparation will be reported elsewhere. Orange plate-like crystals were obtained from an aqueous methanol solution.

**Change of Cell Dimensions Observed by Four-Circle Diffractometer.** A crystal was mounted on a Rigaku AFC-4 four-circle diffractometer, which was covered with black paper to shut off the room light. Cell dimensions were measured accurately using 20 reflections in the range of  $28^\circ < 2\theta < 30^\circ$ .

Crystal data at the initial stage at 293 K are as follows;  $C_{27}H_{36}O_8N_4PCo$ ; fw=634.51;  $a=13.678(2)$ ,  $b=24.880(6)$ ,  $c=9.391(2)$  Å,  $\beta=107.99(1)^\circ$ ;  $V=3040(1)$  Å<sup>3</sup>; space group  $P2_1$ ;  $Z=4$ ;  $d_x=1.39$  g cm<sup>-3</sup>;  $\mu(Mo K\alpha)=6.95$  cm<sup>-1</sup>.

It was found that the cell dimensions were significantly changed when the black paper was removed. To measure the reaction rate, a crystal was mounted on the diffractometer covered with black paper and was irradiated with visible light, which was brought to the crystal from a xenon lamp (Super Bright 150) using a glass fiber tube, the distance between the top of the tube and the crystal being 19.5 cm. The cell dimensions were measured continuously at constant intervals using the 20 reflections. About 40 min are necessary for one cycle of the cell measurement. Figure 1 shows the changes of  $a$ ,  $b$ ,  $c$ ,  $\beta$ , and  $V$  with exposure time. After about 12 h of exposure the changes came within experimental error. The values of  $a$ ,  $b$ ,  $c$ ,  $\beta$ , and  $V$  converged to 13.56(1), 25.06(1), 9.381(6) Å, 107.35(6)°, and 3044(3) Å<sup>3</sup>, respectively.

The variation curves of cell dimensions are well explained by first order kinetics. For example, a log plot of the change of the  $a$  axis length, which showed the largest variation among the five cell parameters, is shown in Fig. 2. The rate constant was calculated to be  $1.3 \times 10^{-4}$  s<sup>-1</sup>, which is greater by about 100 times than that of the racemization of the chiral ce group by X-ray exposure reported so far,

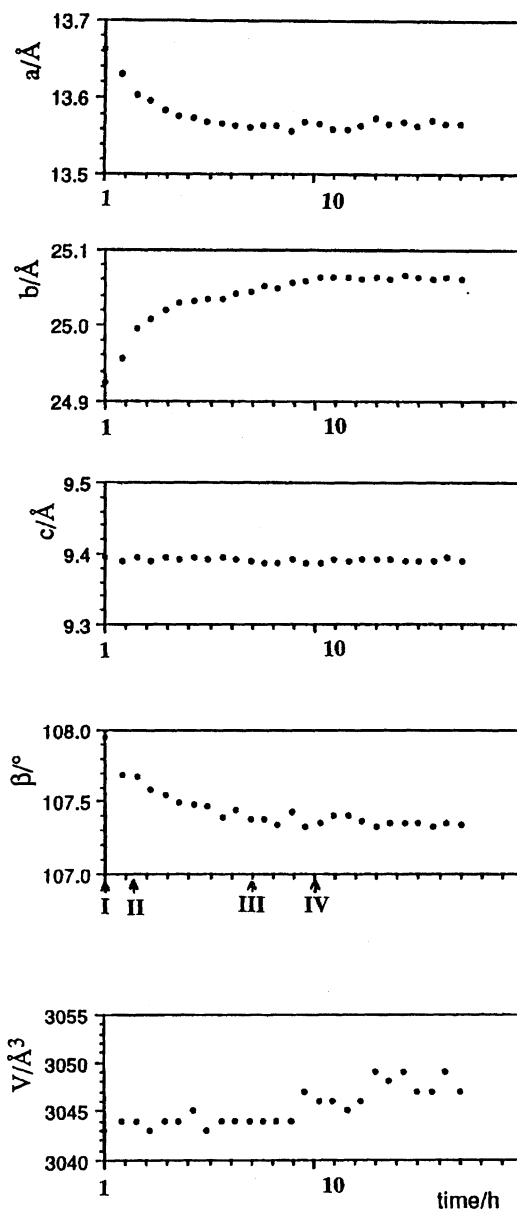


Fig. 1. The change of the unit-cell dimensions on exposure to a xenon lamp observed by the four-circle diffractometer. About 1 h was necessary before the first data set was obtained. The stages I to IV observed by IPD-WAS correspond to the times indicated by arrows.

but is smaller by 200 times than that in the suspended state observed for this complex.<sup>9)</sup>

The intensities of  $h0l$  reflections with  $h+l=\text{odd}$  gradually decreased. Figure 3 shows the average  $I_t/I_0$  of the 20 reflections with exposure time, where  $I_t$  and  $I_0$  mean the intensities at  $t$  h and the initial stage. This indicates that the space group is transformed from the non-centrosymmetric  $P2_1$  to centrosymmetric  $P2_1/n$  in the change of cell dimensions. Such a racemization was classified in the second mode for the crystalline-state racemization of the chiral ce group.<sup>4)</sup> The intensity change may be expressed as first order kinetics although the plots at early stages significantly deviate from the first-order-kinetics curve. This is caused

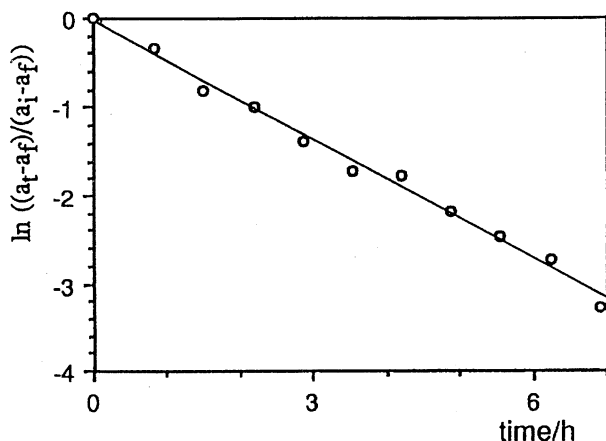


Fig. 2. Log plots of the change of the  $a$  axis length. The value of  $a_i$ ,  $a_f$ , and  $a_t$  means the  $a$  axis length at the initial, final, and  $t$  h.

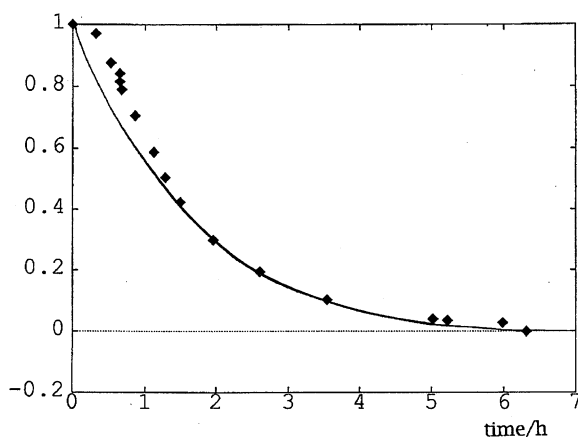


Fig. 3. Decrease in average intensity of  $h0l$  reflections with  $k+l=\text{odd}$ . Several data at early stages are ignored in drawing the curve.

by the intensities of most reflections gradually increasing in the early stages, probably due to the improvement of the crystallinity. Such a change was sometimes observed when a photoreaction occurred in a crystal. The details will be reported elsewhere. The rate constant is approximately the same as that obtained from the cell change.

**Stepwise Data Collection by a New Diffractometer.** Since about 100 h are necessary for the three-dimensional intensity data collection with the usual four-circle diffractometer, it seemed difficult to analyze the structures at several intermediate stages, although the change was slow on exposure to X-rays without photoirradiation. A new diffractometer using an imaging plate (IPD-WAS) was developed by two of us (N. Kamiya and H. Iwasaki) to obtain the three-dimensional intensity data within an hour.<sup>10)</sup> The diffractometer consists of a rotating anode generator, a Weissenberg type camera with several adjustable screens to take reflections in different layers simultaneously, two imaging plates as the detector to read the intensities recorded on one of the plates when another is used for the detector and the reader using a He-Ne laser. The performance and quality of the diffractometer will be reported in detail separately.<sup>10)</sup>

A crystal of  $0.60 \times 0.50 \times 0.40$  mm was mounted on the IPD-WAS diffractometer, which was not covered with black paper. The racemization gradually occurred because of the room light although the rate of the change was about one tenth of the above value obtained by a xenon lamp. Graphite monochromated Mo  $K\alpha$  radiation (60 kV, 300 mA) was used. The  $c$  axis was aligned since it is the shortest one. To obtain the three-dimensional data, the range of rotation around the  $c$  axis,  $180^\circ$ , was divided into 6 parts,  $-142.8^\circ$ — $-113.8^\circ$ ,  $-114.8^\circ$ — $-85.8^\circ$ ,  $-86.8^\circ$ — $-57.8^\circ$ ,  $-58.8^\circ$ — $-29.8^\circ$ ,  $-30.8^\circ$ — $-1.8^\circ$ , and  $-2.8^\circ$ — $-26.2^\circ$  and a Weissenberg photograph was taken in each range. The oscillation speed was  $30^\circ \text{ min}^{-1}$  and the number of oscillations was 10. This requires 19.3 min for one photograph and about 2 h are necessary for obtaining a whole set of three-dimensional intensity data. The merging  $R$  factor was 0.022. The reflections of  $2\theta$  less than  $45^\circ$  were obtained in the range of  $-16 \leq h \leq 13$ ,  $0 \leq k \leq 26$ , and  $0 \leq l \leq 8$ . A total of 4086 unique reflections were obtained, of which 3487 with  $|F_o| > 3\sigma(F_o)$  were used for the structural analysis. The corrections of Lorentz and polarization were applied but those of absorption and extinction were ignored.

**Structure Analysis.** The structure was solved by a direct method with the program MULTAN78<sup>14)</sup> and refined by full-matrix least-squares method with SHELX76.<sup>15)</sup> All the non-hydrogen atoms were refined with anisotropic temperature factors. The distances and angles in the bmce and phenyl groups were constrained to have ideal values. The positions of the hydrogen atoms were calculated geometrically and refined with the fixed isotropic temperature factors. The weighting scheme is  $[\sigma(F_o)^2 + 0.004F_o^2]^{-1}$ . The crystal data and refinement details are summarized in Table 1. Final atomic parameters at stage I are listed in Table 2.

The 20 sets of the three-dimensional intensity data were collected successively in the same conditions. To compare the significant changes in the structure of the chiral bmce group with each other, the first data set described above and the 8th, 15th, and 20th data sets were selected and the crystal structures for four data sets were analyzed. Here-

Table 1. Crystal Data and Details of Refinement at the Four Stages

	Stage I	Stage II	Stage III	Stage IV
$a/\text{\AA}$	13.678(2)	13.621	13.555	13.550
$b/\text{\AA}$	24.880(6)	24.894	24.989	25.014
$c/\text{\AA}$	9.391(2)	9.392	9.389	9.392
$\beta/^\circ$	107.99(1)	107.852	107.458	107.321
$V/\text{\AA}^3$	3040(1)	3031.31	3033.80	3038.96
No. of independent reflections	4086	4092	4024	3931
No. of parameters	739	720	755	360
No. of reflections used in refinement	3487	3467	3883	2890
$S$	1.037	1.079	0.464	0.621
$(\Delta/\sigma)_{\text{max}}$	0.18	0.39	0.46	0.26
$(\Delta\rho)_{\text{min}}/\text{e \AA}^{-3}$	-0.39	-0.74	-0.36	-0.55
$(\Delta\rho)_{\text{max}}/\text{e \AA}^{-3}$	0.92	0.42	0.63	0.72
$R$	0.047	0.055	0.060	0.066
$wR$	0.045	0.054	0.066	0.071

Table 2. Final Atomic Parameters for the Stage I

Atom	<i>x</i>	<i>y</i>	<i>z</i>	<i>B</i> <sub>eq</sub> /Å <sup>2</sup>	Atom	<i>x</i>	<i>y</i>	<i>z</i>	<i>B</i> <sub>eq</sub> /Å <sup>2</sup>
Co1A	0.50769 (6)	0.01464 (4)	-0.22145 (9)	2.57 (2)	Co1B	0.02825 (6)	0.25000	0.31044 (9)	2.41 (2)
N1A	0.4647 (4)	0.0223 (2)	-0.0519 (6)	2.7 (2)	N1B	0.0382 (4)	0.1750 (2)	0.3406 (7)	3.1 (2)
N2A	0.5364 (4)	0.0884 (2)	-0.1804 (7)	3.0 (2)	N2B	-0.0187 (4)	0.2475 (2)	0.4774 (6)	2.8 (2)
N3A	0.5480 (4)	0.0094 (3)	-0.3951 (6)	3.5 (2)	N3B	0.0221 (4)	0.3255 (2)	0.2827 (6)	2.8 (2)
N4A	0.4858 (4)	-0.0589 (2)	-0.2546 (6)	3.1 (2)	N4B	0.0725 (4)	0.2554 (2)	0.1394 (6)	2.8 (2)
O1A	0.4285 (4)	-0.0206 (2)	0.0101 (6)	3.8 (2)	O1B	0.0737 (4)	0.1426 (2)	0.2530 (6)	3.8 (2)
O2A	0.5747 (4)	0.1203 (2)	-0.2676 (7)	4.6 (2)	O2B	-0.0481 (3)	0.2905 (2)	0.5373 (5)	3.5 (1)
O3A	0.5793 (4)	0.0524 (2)	-0.4577 (6)	4.6 (2)	O3B	-0.0065 (3)	0.3596 (2)	0.3753 (5)	3.4 (1)
O4A	0.4492 (4)	-0.0901 (2)	-0.1662 (6)	3.9 (2)	O4B	0.0971 (4)	0.2108 (2)	0.0713 (6)	3.9 (2)
C1A	0.4699 (5)	0.0684 (3)	0.0095 (8)	3.1 (2)	C1B	0.0087 (5)	0.1564 (3)	0.4476 (8)	3.0 (2)
C2A	0.5112 (5)	0.1088 (3)	-0.0692 (8)	3.5 (2)	C2B	-0.0250 (5)	0.1994 (3)	0.5331 (8)	3.4 (2)
C3A	0.5450 (6)	-0.0391 (3)	-0.4489 (9)	4.1 (2)	C3B	0.0502 (6)	0.3443 (3)	0.1747 (9)	3.7 (2)
C4A	0.5076 (5)	-0.0794 (3)	-0.3695 (8)	3.0 (2)	C4B	0.0775 (5)	0.3019 (3)	0.0841 (8)	3.3 (2)
C5A	0.4372 (7)	0.0793 (4)	0.145 (1)	5.4 (3)	C5B	0.0073 (7)	0.0984 (3)	0.484 (1)	4.8 (3)
C6A	0.5219 (7)	0.1672 (3)	-0.029 (1)	5.3 (3)	C6B	-0.0636 (6)	0.1905 (3)	0.6605 (9)	4.3 (3)
C7A	0.5784 (8)	-0.0505 (5)	-0.585 (1)	6.5 (4)	C7B	0.0533 (8)	0.4033 (3)	0.142 (1)	5.4 (3)
C8A	0.4951 (7)	-0.1371 (3)	-0.407 (1)	5.8 (3)	C8B	0.1106 (7)	0.3105 (4)	-0.053 (1)	5.2 (3)
P1A	0.3430 (1)	0.04031 (7)	-0.3747 (2)	2.97 (5)	P1B	-0.1379 (1)	0.23404 (6)	0.1505 (2)	2.67 (5)
C15A	0.3500 (7)	0.0961 (3)	-0.495 (1)	4.7 (3)	C15B	-0.1365 (6)	0.1813 (3)	0.0194 (9)	4.1 (2)
C16A	0.2615 (5)	0.0647 (2)	-0.2658 (8)	3.3 (2)	C16B	-0.2250 (5)	0.2091 (2)	0.2488 (7)	2.9 (2)
C17A	0.2073 (5)	0.0286 (3)	-0.2073 (8)	3.9 (2)	C17B	-0.2768 (5)	0.2446 (3)	0.3146 (9)	4.4 (3)
C18A	0.1489 (7)	0.0457 (3)	-0.119 (1)	5.7 (3)	C18B	-0.3379 (6)	0.2242 (3)	0.3964 (9)	4.5 (3)
C19A	0.1460 (7)	0.1000 (3)	-0.089 (1)	6.1 (4)	C19B	-0.3480 (6)	0.1698 (3)	0.415 (1)	5.1 (3)
C20A	0.1996 (6)	0.1366 (4)	-0.145 (1)	6.1 (3)	C20B	-0.2968 (6)	0.1350 (3)	0.3494 (9)	4.5 (3)
C21A	0.2578 (5)	0.1189 (3)	-0.2339 (8)	4.2 (2)	C21B	-0.2358 (5)	0.1537 (3)	0.2650 (7)	3.6 (2)
C22A	0.2628 (5)	-0.0092 (3)	-0.4997 (7)	3.5 (2)	C22B	-0.2075 (5)	0.2891 (3)	0.0361 (7)	3.5 (2)
C23A	0.2016 (7)	0.0056 (4)	-0.6419 (8)	5.6 (3)	C23B	-0.2655 (8)	0.2795 (4)	-0.1119 (8)	6.8 (3)
C24A	0.135 (1)	-0.0310 (5)	-0.737 (1)	8.6 (5)	C24B	-0.318 (1)	0.3211 (4)	-0.205 (1)	10.4 (6)
C25A	0.1293 (8)	-0.0829 (4)	-0.688 (1)	7.6 (5)	C25B	-0.3181 (9)	0.3723 (4)	-0.143 (1)	8.1 (4)
C26A	0.1909 (6)	-0.0976 (3)	-0.546 (1)	5.2 (3)	C26B	-0.2625 (6)	0.3817 (3)	0.0034 (9)	5.1 (3)
C27A	0.2561 (5)	-0.0617 (3)	-0.4498 (8)	3.9 (2)	C27B	-0.2100 (5)	0.3399 (2)	0.0921 (8)	3.7 (2)
C9A	0.6569 (4)	-0.0065 (2)	-0.0873 (6)	3.0 (2)	C9B	0.1754 (4)	0.2583 (3)	0.4615 (6)	3.6 (2)
C10A	0.7347 (5)	0.0292 (2)	-0.1127 (7)	3.6 (2)	C10B	0.2512 (5)	0.2629 (2)	0.3822 (8)	4.1 (2)
O5A	0.7713 (5)	0.0673 (2)	-0.0366 (8)	6.8 (2)	O5B	0.2799 (4)	0.3054 (2)	0.3477 (8)	6.0 (2)
O6A	0.7658 (4)	0.0152 (2)	-0.2313 (6)	5.2 (2)	O6B	0.2833 (4)	0.2164 (2)	0.3389 (7)	5.5 (2)
C11A	0.8305 (9)	0.0523 (5)	-0.276 (1)	9.4 (6)	C11B	0.3499 (8)	0.2194 (5)	0.247 (1)	8.0 (5)
C12A	0.6709 (4)	-0.0113 (3)	0.0772 (6)	4.2 (3)	C12B	0.1908 (4)	0.2995 (3)	0.5812 (7)	4.0 (2)
C13A	0.7728 (5)	-0.0317 (3)	0.1627 (6)	4.1 (3)	C13B	0.2870 (5)	0.2933 (3)	0.7039 (8)	4.8 (3)
O7A	0.8319 (5)	-0.0551 (3)	0.1141 (7)	6.7 (2)	O7B	0.3325 (8)	0.2521 (3)	0.736 (1)	14.3 (4)
O8A	0.7982 (4)	-0.0214 (3)	0.3106 (5)	5.6 (2)	O8B	0.3214 (6)	0.3375 (3)	0.7816 (8)	8.6 (3)
C14A	0.8902 (7)	-0.0458 (5)	0.4062 (9)	7.4 (4)	C14B	0.409 (1)	0.3344 (6)	0.911 (1)	11.1 (6)

after, the stages at which the first, 8th, 15th, and 20th data sets were obtained are called the stages I, II, III, and IV, respectively. Although the cell dimensions for each data set were obtained from the  $2\theta$  values of more than 50 reflections, the accuracy is not as good as that of the cell dimensions obtained by a four-circle diffractometer because of the poor accuracy of the  $2\theta$  value in the Weissenberg method. The cell dimensions of four stages correspond to those indicated by arrows in the conversion curves of Fig. 1. The decrease in the average intensity of the reflections that disappear due to extinction of the racemic crystal is in fair agreement with the change of cell dimensions.

The structures at other stages were analyzed in similar ways to that of stage I described above. At stage II the disordered atoms of C(12B), C(13B), O(7B), O(8B), C(14B), O(7'B), and O(8'B) were refined with isotropic temperature factors. The occupancy factors of the disordered atoms were refined to have the same isotropic temperature factors. The

positions of the hydrogen atoms were obtained geometrically and refined with the fixed isotropic temperature factors. The distances and angles of the bmce group and the phenyl groups were fixed to have ideal values. The other refinement details are also listed in Table 1.

At stage III the refinement was very difficult since the intensity of  $h0l$  reflections with  $h+l=\text{odd}$  became very weak. This indicates that the space group changed from  $P2_1$  to  $P2_1/n$  in the process of racemization and that the two crystallographically independent molecules are closely related by an inversion center. Further refinement, therefore, was done, regarding the space group as  $P2_1/n$ . The disordered atoms appeared around another methoxycarbonyl group in addition to the disordered methoxycarbonyl group observed in stage II. The original atoms, C(10), O(5), O(6), and the newly appearing ones, C(10'), O(5'), and O(6'), were refined to have the same isotropic temperature factors. The somewhat large  $R$  value is probably due to the inappropri-

ate space group. The other conditions of the refinement are the same as those at stage II. The details of the refinement are given in Table 1.

At stage IV the disordered structure of the methoxycarbonyl group observed in stage II had disappeared, but another methoxycarbonyl group bonded to the chiral carbon atom has still disordered structure. The occupancy factors were refined to have the same isotropic temperature factors and became 80:20. The other conditions were the same as those at stage III. The refinement details are listed in Table 1. The final atomic parameters are listed in Table 3. Tables of atomic parameters for non-H atoms at stages II and III, and atomic parameters for H atoms, anisotropic thermal parameters for non-H atoms, bond distances, bond angles and torsion angles, and  $F_o - F_c$  tables at four stages were deposited as Document No. 68049 at the Office of the Editor of Bull. Chem. Soc. Jpn.

## Results and Discussion

**Structure at Stage I.** The crystal structure viewed along the  $c$  axis at stage I is shown in Fig. 4. There are two crystallographically independent molecules, A and B, in an unit cell. The two molecules are closely related by a pseudo inversion center,  $i'$ , except for the chiral bmce groups. The chiral bmce groups of the two molecules touch each other. There is no short contact between the molecules. The molecular structures of A and B are shown in Fig. 5. The cobaloxime moieties and phosphine ligands of the two molecules are mirror images of each other. The selected bond distances and angles are listed in Table 4. These val-

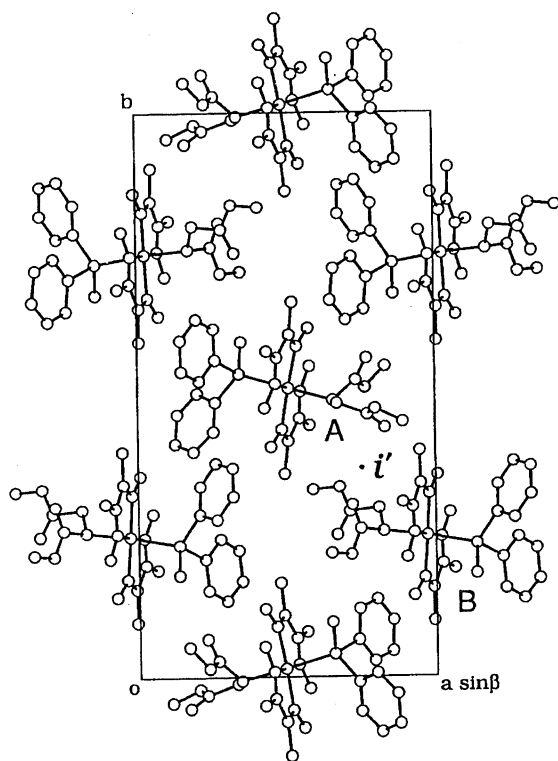


Fig. 4. Crystal structure viewed along the  $c$  axis at stage I.

Table 3. Final Atomic Parameters for the Stage IV

Atom	$x$	$y$	$z$	$B$ or $B_{eq}/\text{\AA}^2$
Co1	0.22641 (6)	0.37113 (3)	0.94551 (9)	2.98 (3)
N1	0.2014 (4)	0.2977 (2)	0.9034 (6)	3.8 (2)
N2	0.2720 (4)	0.3666 (2)	0.7765 (6)	3.3 (2)
N3	0.2460 (4)	0.4444 (2)	0.9816 (6)	3.4 (2)
N4	0.1836 (4)	0.3753 (2)	1.1184 (7)	3.9 (2)
O1	0.1615 (4)	0.2656 (2)	0.9881 (6)	5.1 (2)
O2	0.3079 (3)	0.4091 (2)	0.7188 (5)	4.3 (2)
O3	0.2791 (4)	0.4775 (2)	0.8927 (5)	4.5 (2)
O4	0.1524 (4)	0.3321 (2)	1.1799 (6)	5.1 (2)
C1	0.2297 (5)	0.2786 (3)	0.7923 (8)	3.8 (2)
C2	0.2705 (5)	0.3195 (3)	0.7171 (7)	3.8 (2)
C3	0.2236 (5)	0.4635 (3)	1.0975 (8)	4.0 (2)
C4	0.1878 (5)	0.4222 (3)	1.1805 (8)	3.8 (2)
C5	0.2236 (7)	0.2211 (3)	0.756 (1)	5.8 (3)
C6	0.3094 (6)	0.3093 (3)	0.5853 (9)	5.4 (3)
C7	0.2322 (8)	0.5212 (3)	1.138 (1)	6.4 (3)
C8	0.1541 (8)	0.4314 (4)	1.314 (1)	6.8 (3)
P1	0.3912 (1)	0.34712 (6)	1.0986 (2)	3.27 (5)
C15	0.3834 (6)	0.2925 (3)	1.2205 (8)	5.1 (3)
C16	0.4757 (5)	0.3219 (3)	0.9944 (7)	3.6 (2)
C17	0.5313 (6)	0.3571 (3)	0.9330 (9)	4.6 (2)
C18	0.5905 (6)	0.3381 (3)	0.8460 (9)	5.6 (3)
C19	0.5948 (6)	0.2846 (4)	0.821 (1)	6.0 (3)
C20	0.5401 (6)	0.2491 (3)	0.880 (1)	5.6 (3)
C21	0.4799 (5)	0.2675 (3)	0.9671 (8)	4.5 (2)
C22	0.4691 (5)	0.3975 (3)	1.2238 (7)	3.7 (2)
C23	0.5251 (9)	0.3854 (4)	1.368 (1)	7.5 (4)
C24	0.586 (1)	0.4233 (5)	1.459 (1)	11.2 (5)
C25	0.589 (1)	0.4748 (5)	1.407 (1)	9.6 (5)
C26	0.5365 (6)	0.4869 (3)	1.269 (1)	5.8 (3)
C27	0.4769 (5)	0.4495 (3)	1.1761 (8)	4.4 (2)
C9	0.0785 (4)	0.3934 (2)	0.8149 (6)	4.1 (2)
C10	-0.0018 (8)	0.3594 (3)	0.843 (1)	6.4 (1) <sup>a</sup>
O5	-0.0383 (5)	0.3222 (2)	0.7625 (7)	6.4 (1) <sup>a</sup>
O6	-0.0334 (5)	0.3706 (3)	0.9623 (7)	6.4 (1) <sup>a</sup>
C11	-0.1059 (8)	0.3373 (4)	1.001 (1)	6.4 (1) <sup>a</sup>
C12	0.0627 (4)	0.3977 (4)	0.6500 (6)	6.4 (3)
C13	-0.0391 (5)	0.4156 (4)	0.5598 (6)	6.6 (3)
O7	-0.0962 (6)	0.4412 (4)	0.6088 (8)	12.1 (4)
O8	-0.0670 (5)	0.4043 (3)	0.4127 (6)	9.9 (3)
C14	-0.1560 (8)	0.4308 (5)	0.3184 (9)	11.5 (5)
C109	0.002 (3)	0.3820 (6)	0.893 (4)	6.4 (1) <sup>a</sup>
O59	-0.026 (2)	0.4174 (7)	0.959 (3)	6.4 (1) <sup>a</sup>
O69	-0.036 (2)	0.3326 (6)	0.889 (3)	6.4 (1) <sup>a</sup>
C119	-0.087 (3)	0.316 (1)	0.995 (4)	6.4 (1) <sup>a</sup>

a) These atoms were refined isotropically.

ues are not significantly different from the corresponding ones observed in the related complexes. The bmce groups of the A and B molecules take an L type conformation and have similar torsion angles around the C-C single bonds; the torsion angles of C(10)-C(9)-C(12)-C(13) are  $-58.4(8)$  and  $-65.7(7)^\circ$  for A and B, respectively, and the torsion angles of C(12)-C(9)-C(10)-O(5) and C(9)-C(12)-C(13)-O(17) are  $32(1)$  and  $41(1)^\circ$ , and  $-20(1)$  and  $-31(1)^\circ$  for A and B, respectively. On the other hand, the conformation around the Co-C bond is different by about  $40^\circ$  between the

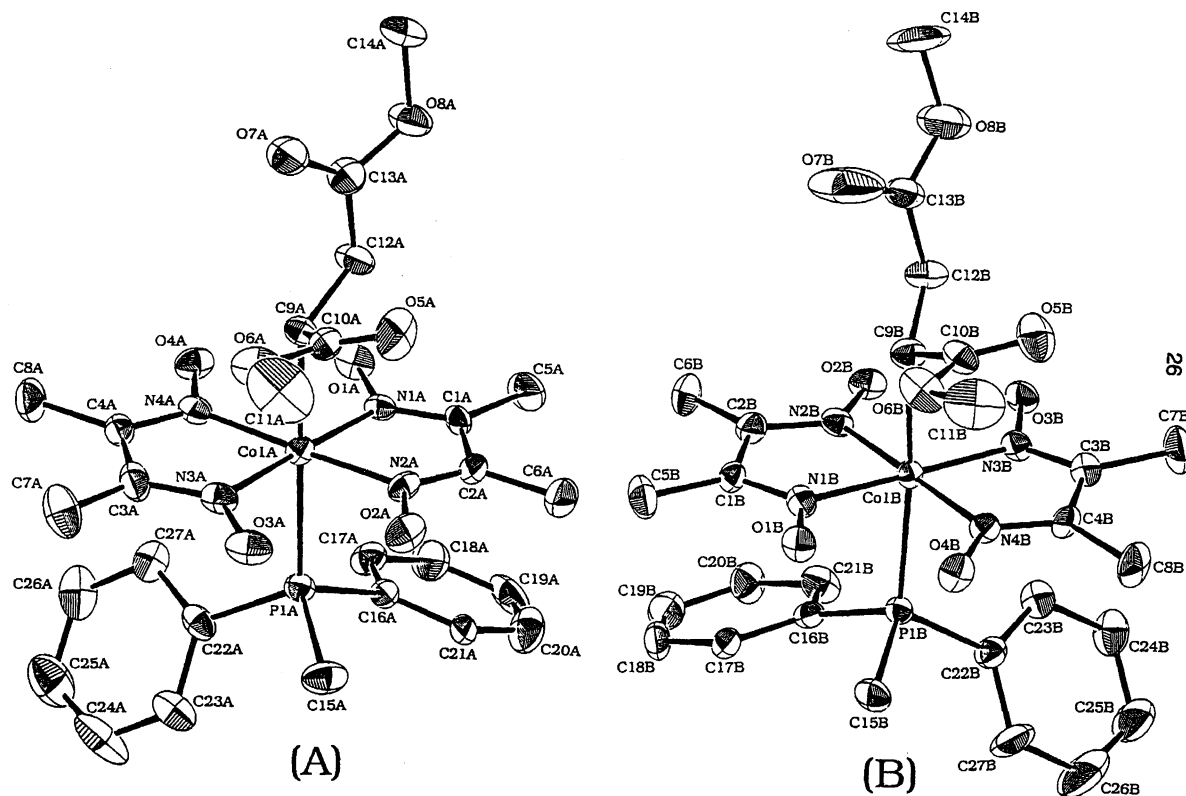


Fig. 5. Molecular structures of (a) A and (b) B at stage I.

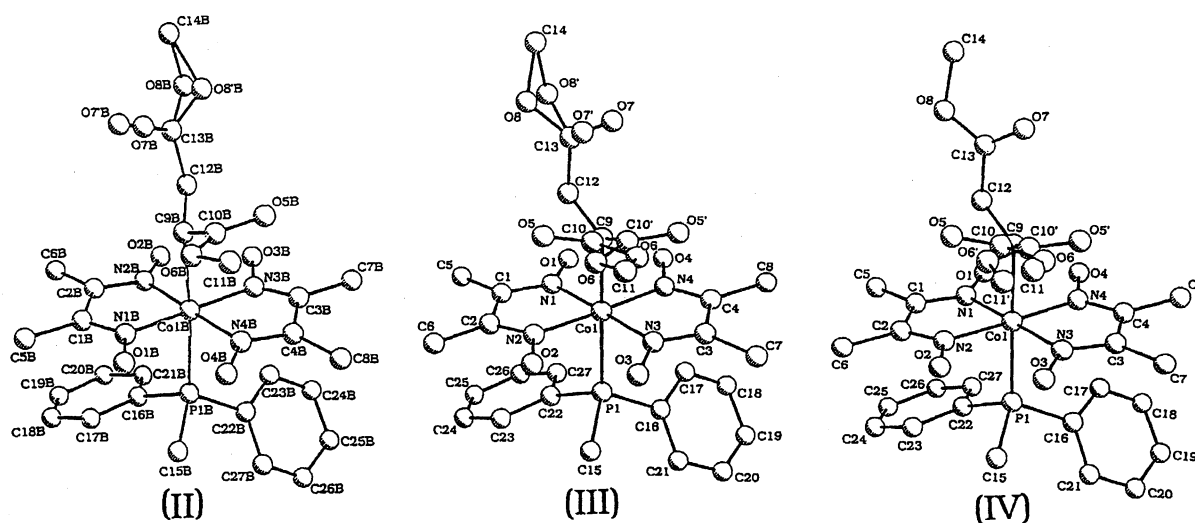


Fig. 6. Molecular structures of B at stages (a) II, (b) III, and (c) IV.

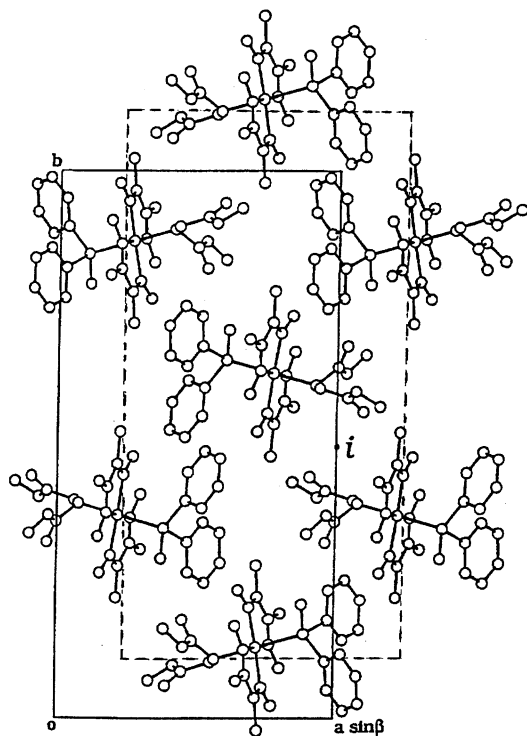
two molecules; the torsion angles of N(2A)-Co(1A)-C(9A)-C(10A) and N(4B)-Co(1B)-C(9B)-C(10B) are  $-42.9(6)$  and  $-1.7(5)^\circ$ , respectively.

**Structure at Stage II.** The crystal structure at stage II is in good agreement with that in stage I except that the bmce group of the B molecule (B bmce group) has a disordered structure. Figure 6(a) shows the molecular structure of B. The methoxycarbonyl group with nearly perpendicular conformation to the cobaloxime plane takes a disordered structure, which is caused

by a rotation around the C(12B)-C(13B) bond. The occupancy factors of the original methoxycarbonyl group, C(13B), O(7B), O(8B), and C(14B) and the newly appearing group, C(13B), O(7'B), O(8'B), and C(14B) are 0.59(2) and 0.41(2), respectively. The torsion angles of C(9B)-C(12B)-C(13B)-O(7B) and C(9B)-C(12B)-C(13B)-O(7'B) are  $-19(2)$  and  $-67(2)^\circ$ , respectively. The former is the same within experimental error as that at stage I. The A molecule is approximately the same as that at the stage I.

Table 4. Selected Bond Distances (Å) at the Stage I

Bond	A molecule	B molecule
Co-N1	1.892(5)	1.885(5)
Co-N2	1.869(6)	1.871(6)
Co-N3	1.864(6)	1.893(5)
Co-N4	1.881(7)	1.888(6)
Co-P1	2.354(2)	2.337(2)
Co-C9	2.105(5)	2.082(5)
P1-C15	1.812(9)	1.803(8)
P1-C16	1.832(8)	1.826(8)
P1-C22	1.817(6)	1.817(6)

Fig. 7. Crystal structure viewed along the *c* axis at stage IV.

**Structure at Stage III.** The crystal structure was solved assuming a centrosymmetric space group. This means that the counterpart of the A molecule appears at the B molecule site and vice versa. We must subtract the counterpart of the inverted molecule from the obtained disordered structure. Figure 6(b) shows the molecular structure at the B molecular site. Both of the methoxycarbonyl groups take disordered structures. For the perpendicular group the torsion angles of C(9)–C(12)–C(13)–O(7) and C(9)–C(12)–C(13)–O(7') are 31(1) and  $-24(2)^\circ$ , respectively, and the occupancy factors of the methoxycarbonyl groups composed of C(13), O(7), O(8), and C(14) and C(13), O(7'), O(8'), and C(14) are 0.80(1) and 0.20(1), respectively. This indicates that the true composition of the former and latter groups at the B molecular site are 0.30 and 0.20, respectively, since the methoxycarbonyl group of C(13), O(7), O(8), and C(14) is the inverted one of the

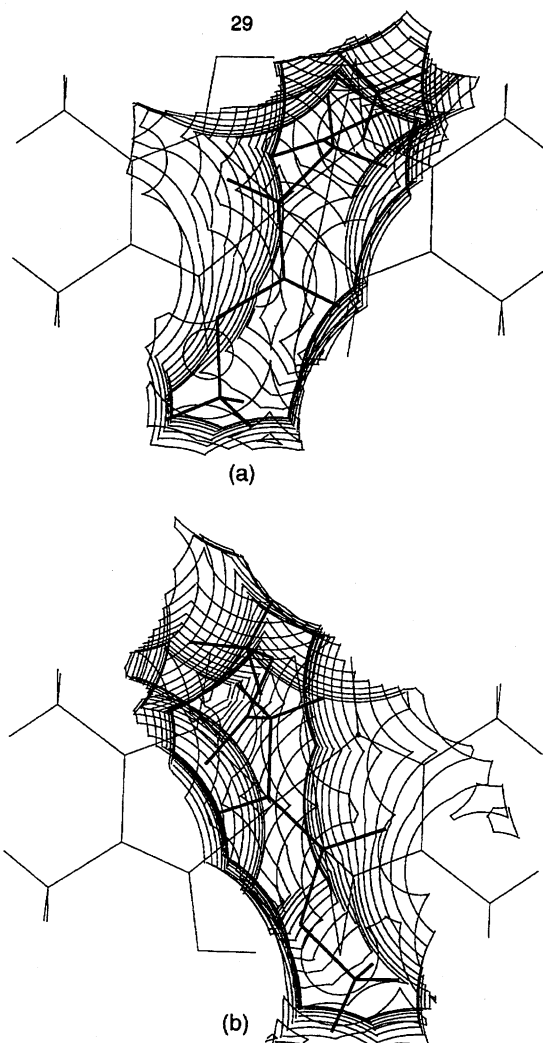


Fig. 8. Reaction cavities for the A and B bmce groups viewed along the normal to the cobaloxime plane.

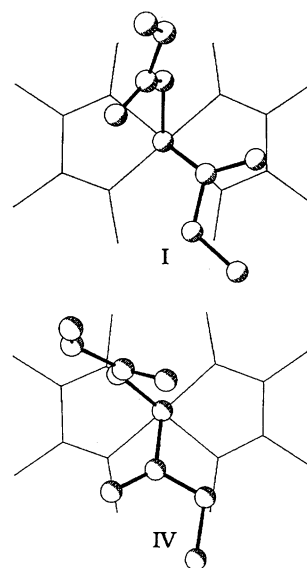


Fig. 9. Conformational and configurational change of the B bmce group from stage I to IV.

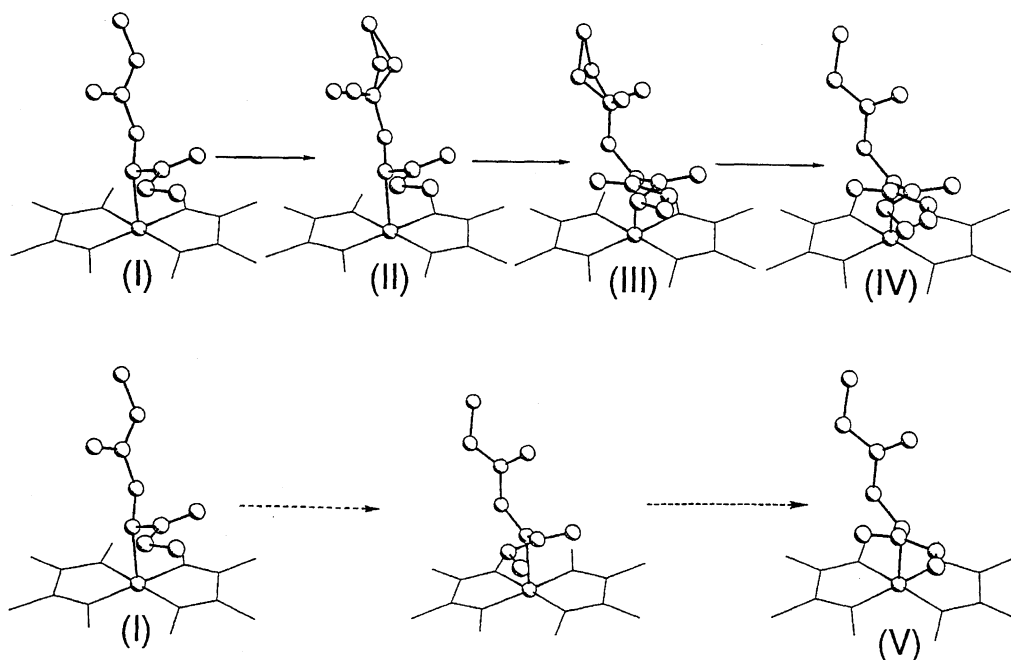


Fig. 10. Inversion process of the B bmce group.

A molecule, that is, the counterpart of the A molecule.

Another methoxycarbonyl group, which is nearly parallel to the cobaloxime plane, have a disordered structure. The torsion angles of  $N(3)-Co(1)-C(9)-C(10)$  and  $N(3)-Co(1)-C(9)-C(10')$  are  $-51.3(6)$  and  $-15.8(7)^\circ$ , respectively. The occupancy factors of the methoxycarbonyl groups composed of  $C(10)$ ,  $O(5)$ ,  $O(6)$ , and  $C(11)$ , and  $C(10')$ ,  $O(5')$ ,  $O(6')$ , and  $C(11')$  are 0.80 and 0.20, respectively. The original A molecule has the torsion angle of  $55.8(5)^\circ$ , the true compositions of the methoxycarbonyl groups with parallel conformation are 0.30 and 0.20.

**Structure at Stage IV.** The molecular structure at the B site at stage IV is shown in Fig. 6(c). The methoxycarbonyl group with the perpendicular conformation takes an ordered structure, while that of parallel conformation has a disordered structure. The occupancy factors of the major ( $C(10)$ ,  $O(5)$ ,  $O(6)$ , and  $C(11)$ ) and minor ( $C(10')$ ,  $O(5')$ ,  $O(6')$ , and  $C(11')$ ) groups are 0.80 and 0.20, respectively. The torsion angles of the major and minor groups,  $N(3)-Co-C(9)-C(10)$ , are  $-52.2(6)$  and  $-24(1)^\circ$ , respectively. Although the B bmce group was not completely inverted at stage IV, it should be fully inverted after the infinite exposure, because the space group was changed to a centrosymmetric one and the A bmce group should be non-reactive. The final stage V is assumed to have an complete inversion center and the ordered bmce group.

The crystal structure at stage IV is shown in Fig. 7, in which the minor part of the disordered bmce group is omitted for clarity. The ordered chiral structure is changed to an ordered racemic one. Such a process is classified as mode II in the racemization of the ce group. The crystals of the ce complexes with pyridine,<sup>16)</sup> 4-

cyanopyridine,<sup>5)</sup> and 4-methylpyridine<sup>17)</sup> as axial base ligands are belonging to mode II.

**Cavities for the A and B bmce Groups.** To discover the reason why only the B bmce group is inverted, the cavities for the A and B bmce groups at stage I were calculated, and are shown in Fig. 8. The integrated volumes are 47.4 and 55.0 Å<sup>3</sup> for the A and B bmce groups, respectively. It is clear that the B bmce group, with the larger cavity, is inverted. For the ce complex crystals unequal cavities for the two crystallographically independent ce groups were observed and the ce groups with larger cavities are inverted to have the opposite configuration.<sup>16)</sup> The concept of the cavity is applicable even for such a bulky group.

**Conformational and Configurational Changes of the B bmce Group.** On exposure to visible light, only the B bmce group was inverted to have the opposite configuration, retaining the single crystal form. Figure 9 shows the conformational and configurational change of the B bmce group in the process of inversion. The methoxycarbonyl group with perpendicular conformation rotates counterclockwise by about  $50^\circ$  around the  $C(12)-C(13)$  bond. The bmce group rotates counterclockwise by about  $40^\circ$  around the  $Co-C(9)$  bond. And the methoxycarbonyl group with parallel conformation is inverted to have the opposite configuration, following the rotation by about  $180^\circ$  around the  $C(9)-C(10)$  bond. This must be the least motion of the atoms when the bulky bmce group takes the inverted configuration in the crystalline lattice.

Such a large motion of the B bmce group cannot occur simultaneously without degradation of the crystallinity. The stepwise motion of the B bmce group is summarized in Fig. 10. At stage II, the perpendicular



methoxycarbonyl group librates around the C(12)–C(13) bond. The torsion angle of C(9)–C(12)–C(13)–O(7) is varied from  $-31(1)^\circ$  to the range of  $-19(2)^\circ$ – $-67(2)^\circ$ . At stage III, the rotation around the C(12)–C(13) bond occurs and the torsion angle of C(9)–C(12)–C(13)–O(7) is the range of  $-24(2)^\circ$ – $31(1)^\circ$ . Moreover, the methoxycarbonyl group with parallel conformation is partly inverted to the opposite configuration. The ratio of the original *R* configuration to the inverted *S* became 40:60. The libration around the C(12)–C(13) bond may cause the motion of the bmce group in the neighboring A molecule although the A bmce group remained unaltered in X-ray analysis and then the motion may be a trigger of the inversion of the B bmce group since the A and B bmce groups are in contact with each other around the inversion center. It must be emphasized that after most of the perpendicular methoxycarbonyl groups in the B bmce groups changed their conformation, the inversion of the parallel methoxycarbonyl group occurred. At stage IV, the perpendicular methoxycarbonyl group takes an ordered structure and the inversion of the perpendicular methoxycarbonyl group proceeds. After infinite exposure, at stage V, the B bmce group will have an ordered structure as a whole and the true crystallographic inversion center will appear between the A and B bmce groups.

The disordered structures observed at stages II and III clearly indicate that the B bmce group changes its conformation of the perpendicular methoxycarbonyl group in the first step and then is inverted to the opposite configuration. In other word, the B bmce group takes an metastable intermediate structure in the process of the inversion, as shown in Fig. 10.

It is noteworthy that the chiral carbon atom, C(9), in the intermediate structure indicates a  $sp^2$  hybridization. This may suggest that the C=C double bond structure would be made due to hydrogen abstraction from C(9) and C(12) at the intermediate stage. For the ce complexes, the Co–C bond was cleaved by the radiation in the first step and then the cyanoethyl radical would rotate around the C–C–N bond followed by the recombination of the Co–C bond.<sup>3)</sup> Even if the bis(methoxycarbonyl)ethyl radical may be formed by the homolytic Co–C bond cleavage by photoirradiation, it may be too bulky to rotate and face the opposite side to the cobalt atom without destroying the crystalline lattice. The process of the hydrogen abstraction from the chiral carbon and recombination to another site of the chiral carbon may be plausible from the topochemical point of view. Although this model should be examined by the

spectroscopic technique, it is clear that the metastable structure observed by the rapid data collection may be important in the process of inversion.

This work was supported by the Grant-in-Aid on Priority Areas No. 63628003, 01628002, and 02210102 from the Ministry of Education, Science and Culture.

## References

- 1) Part 17: Y. Sakai, Y. Ohashi, M. Yamanaka, Y. Kobayashi, Y. Arai, and Y. Ohgo, *Acta Crystallogr., Sect. B*, **B49**, 1010 (1993).
- 2) Y. Ohashi and Y. Sasada, *Nature*, **267**, 142 (1977).
- 3) Y. Ohashi, K. Yanagi, T. Kurihara, Y. Sasada, and Y. Ohgo, *J. Am. Chem. Soc.*, **103**, 5805 (1981).
- 4) Y. Tomotake, A. Uchida, Y. Ohashi, Y. Sasada, Y. Ohgo, and S. Baba, *Isr. J. Chem.*, **25**, 327 (1985).
- 5) Y. Ohashi, A. Uchida, Y. Sasada, and Y. Ohgo, *Acta Crystallogr., Sect. B*, **B39**, 54 (1983).
- 6) Y. Ohashi, *Acc. Chem. Res.*, **21**, 268 (1988).
- 7) T. Kurihara, Y. Ohashi, Y. Sasada, and Y. Ohgo, *Acta Crystallogr., Sect. B*, **B39**, 243 (1983).
- 8) T. Kurihara, Y. Ohashi, and Y. Sasada, *Acta Crystallogr., Sect. B*, **B38**, 2484 (1982); T. Kurihara, A. Uchida, Y. Ohashi, Y. Sasada, and Y. Ohgo, *J. Am. Chem. Soc.*, **106**, 5718 (1984).
- 9) Y. Ohgo, Y. Arai, and S. Takeuchi, *Chem. Lett.*, **1991**, 455.
- 10) N. Kamiya, I. Tanaka, and H. Iwasaki, "Reactivity in Molecular Crystals," Kodansha-VCH, Tokyo (1993), p. 25; N. Kamiya and H. Iwasaki, *J. Appl. Crystallogr.*, (1995) in press.
- 11) Y. Sakai, Master Thesis, Tokyo Institute of Technology, Tokyo, 1992.
- 12) Y. Sakai, T. Tamura, A. Uchida, Y. Ohashi, E. Hasegawa, Y. Arai, and Y. Ohgo, *Acta Crystallogr., Sect. C*, **C47**, 1196 (1991).
- 13) Y. Ohgo, S. Takeuchi, Y. Natori, J. Yoshimura, Y. Ohashi, and Y. Sasada, *Bull. Chem. Soc. Jpn.*, **54**, 3095 (1981).
- 14) P. Main, L. Lessinger, M. M. Woolfsom, G. Germain, and J. P. Declercq, "MULTAN 78 (A system of computer program for the automatic solution of crystal structures from X-ray diffraction data)," University of York, England and Louvain, Belgium (1978).
- 15) G. M. Sheldrick, "SHELX 76 (A program for crystal structure determination)," University of Cambridge, England (1976).
- 16) Y. Ohashi, K. Yanagi, T. Kurihara, Y. Sasada, and Y. Ohgo, *J. Am. Chem. Soc.*, **104**, 6353 (1982).
- 17) A. Uchida, Y. Ohashi, Y. Sasada, and Y. Ohgo, *Acta Crystallogr., Sect. B*, **B40**, 473 (1984).